Molecular Crystals and Liquid Crystals Science and Technology. Section A. Molecular Crystals and Liquid Crystals
Publication details, including instructions for authors and subscription information:
http://www.tandfonline.com/loi/gmcl19

Molecular/Polymeric Magnets

Arthur J. Epstein [a b] & Joel S. Miller [a b]
[a] Department of Physics and Department of Chemistry, The Ohio State University Columbus, Ohio, 43210-1106, U.S.A.
[b] Science and Engineering Laboratories The Du Pont Company Wilmington, Delaware, 19880-0328, U.S.A.
Version of record first published: 24 Sep 2006.

To cite this article: Arthur J. Epstein & Joel S. Miller (1993): Molecular/Polymeric Magnets, Molecular Crystals and Liquid Crystals Science and Technology. Section A. Molecular Crystals and Liquid Crystals, 228:1, 99-130

To link to this article: http://dx.doi.org/10.1080/10587259308032150

Mol. Cryst. Liq. Cryst. 1993, Vol. 228, pp. 99–130
Reprints available directly from the publisher
Photocopying permitted by license only

Printed in the United States of America

MOLECULAR/POLYMERIC MAGNETS

ARTHUR J. EPSTEIN
Department of Physics and Department of Chemistry
The Ohio State University
Columbus, Ohio 43210-1106 U.S.A.

JOEL S. MILLER
Science and Engineering Laboratories
The Du Pont Company
Wilmington, Delaware 19880-0328 U.S.A.

Abstract The discovery of a transition at 4.8K to a three-dimensional ferromagnetic state in the molecular electron transfer salt $[FeCp^*_2][TCNE]$ and the recent report of ferrimagnetism in the molecular based $V(TCNE)_x \cdot y(CH_2Cl_2)$ adds magnetism to the list of cooperative phenomena now possible in molecular/organic/polymer materials. In this report we review our progress in the study of molecular/polymeric materials that feature a magnetic ground state with a net moment, present a brief discussion of the development of magnetic exchange in these molecular based magnets, and summarize magnetic phenomena in these systems. Emphasis is placed on recent developments in the high T_c molecular magnet systems including the treatment of their magnetic behavior within the framework of a correlated spin glass (CSG)/ferrimagnet with wandering axis (FWA) formalism. The central role of the relative magnitudes of magnetic exchange, randomness in magnetic exchange, magnetic anisotropy, and randomness in magnetic anisotropy is proposed. This latter perspective provides a guide to the controllable synthesis of molecular based magnets of tunable desired properties including high transition temperatures and/or high magnetic susceptibilities.

INTRODUCTION

Magnetic materials have been known to mankind since the discovery of naturally occurring magnets (lodestone) in ancient Greece more than three thousand years ago. Magnets found early application with the invention of the compass by the

Chinese approximately 1500 years ago. However, it was not until the wide spread use of electricity that magnets became important for technological development. The origins of magnetism as based upon quantum mechanical exchange and the role of the Pauli exclusion principle was developed in the 1930's.[1,2] Currently magnets are used in a wide variety of devices ranging from magnetic and magneto-optic memories, to magnetic switches, motors, bearings, etc. The materials in use in today's technologies are transition metal based (e.g., Fe, CrO_2, Fe_2O_3,...) and rare earth metal based (e.g., Co_5Sm, $Co_{17}Sm_2$, $Nd_2Fe_{14}B$,...).[3] Initially molecular and polymer based magnetic materials were thought unlikely, but the discovery of molecular based magnets with transition temperatures in the range of liquid helium in the mid 1980's[4-6], and the report[7-9] of "polymer" magnets with transition temperature above room temperature in 1991 has given an embodiment to the concepts of a molecular/polymeric magnet.[10,11] The molecular based magnets provide a laboratory for the study of a wide range of magnetic phenomena ranging from quasi-one-dimensional effects to the ramifications of random anisotropy and exchange in the three-dimensional coupled hight T_c systems.

MAGNETISM AND MAGNETIC PHENOMENA

Magnetism reflects the alignment of unpaired spins (due to partly occupied atomic or molecular orbitals) in a solid. In the absence of an applied magnetic field, H, the spins point in random directions. In the presence of an applied magnetic field the spins will preferentially align to lower their energy, developing a net magnetic moment. A bulk magnetization develops proportional to the applied field, $M = \chi H$ where χ, is the magnetic susceptibility. When thermal energies (k_BT) are small with respect to the exchange energies (J) the influence of the spins on their neighbors can lead to a net alignment of the spins in the absence of an applied magnetic field. As numerous excellent reviews and introductory articles already exist[1-3], we only outline below several types of magnetic ordering that are known to occur in solids, and, in

particular, are known or suggested to occur in molecular/organic/polymer magnets.

Ferromagnetism

Below the three-dimensional ordering temperature (critical temperature, T_C), the spins within a ferromagnet begin to align to develop a long range order. Well below T_C the spins are completely aligned. Representing individual spins pointing in the vertically up direction by ↑ and a spin pointing vertically downward by ↓ , a ferromagnetic state well below T_C may be represented by:

↑ ↑ ↑ ↑ ↑ ↑ ↑ ↑ ↑

Antiferromagnetism

Under most conditions spins anti align below the critical temperature forming an antiferromagnetic state. There are many topologies within a crystal by which one can get a near zero magnetic moment. Below we show schematically a particularly simple type of antiferromagnetic alignment with nearest neighbor spins pointing in opposite directions:

↑ ↓ ↑ ↓ ↑ ↓ ↑ ↓ ↑

Ferrimagnetism

If the anti aligned spin sites within the magnet have spins of differing magnitude (for example, S = 1/2 and S = 1), then anti alignment of adjacent spins leads to incomplete cancellation of the magnetic moment, forming a ferrimagnetic state, for example:

↑ ↓ ↑ ↓ ↑ ↓ ↑ ↓ ↑

Metamagnetism

Numerous other types of magnetic ordering may be envisioned. For some of these the spin ordering in the solid will change from one ordering pattern to another upon application of a sufficiently large magnetic field. One example of this is the metamagnetic system shown schematically below:

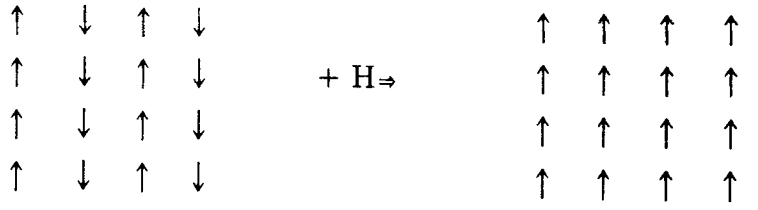

For metamagnets the zero field cooled samples develop an antiferromagnetic order. Upon application of a sufficient large external magnetic field the magnetic state switches to ferromagnetic alignment.

Spin Glass

In a system where there is a substantial disorder there are two limiting types of effects - random exchange (where the strength of interaction among neighboring spins varies between pairs of spins) and random anisotropy (where the preferred spin directions are defined by short-range structural order leading to the appearance of local random anisotropy).[12,13] If the magnitude of the random anisotropy is large compared to the exchange, the local anisotropy field orients the spins essentially along their randomly oriented anisotropy axes, giving rise to a magnetically disordered state, the spin glass (or speromagnetic) state. Though the spins are locally fixed there is no intermediate or long range order and there is no spontaneous magnetization. Exposure to a strong enough external magnetic field may produce a net magnetic order. A schematic arrangement for a spin glass is:

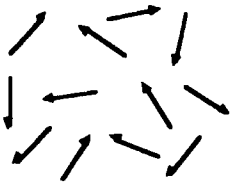

Correlated Spin Glass

In the limit of weak anisotropy, the exchange interaction favors long range magnetic order. However, the random fields can destroy the long range order. At zero applied magnetic field, the magnetization may smoothly vary over a correlation distance forming a correlated spin glass[12,13], shown schematically illustrated for a ferrimagnetic system. The magnetic correlation length in the absence of an applied magnetic field is determined by the strength of the magnetic exchange, the magnitude of the uniaxial anisotropy, and the magnitude of the random anisotropy.

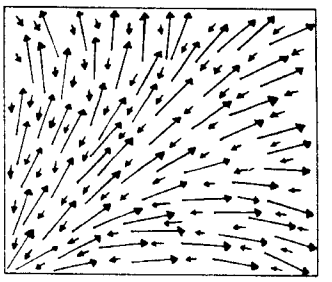

Ferromagnet (ferrimagnet) with Wandering Axis

If a sufficiently strong magnetic field is applied to a correlated spin glass system, then the spins tend to align though there is still some amount of disorder in the direction perpendicular to the direction of the magnetic fields. The resulting state has been called a ferromagnet (or ferrimagnet) with wandering axis (FWA). The presence of some coherent (as opposed to random) anisotropy can also transform the correlated spin glass into a ferromagnet (or ferrimagnet) with wandering axis.[12,13] For example, a ferrimagnet with wandering axis may be viewed as:

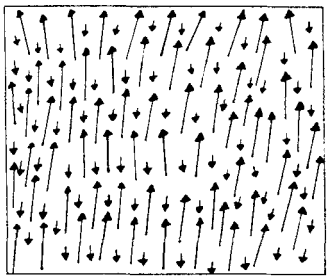

General Hamiltonian for Describing Magnetism

The usual exchange Hamiltonian may be generalized to explicitly study the effects of spin magnitude (S = 1/2, 1, 3/2,...), spin anisotropy (Heisenberg, xy or Ising like spins) and the anisotropy of the exchange between adjacent sites (J_x, J_y, and J_z, where x, y , and z refer to differing crystal directions). Models for the origin of the magnetic exchange in molecular/polymeric magnets are introduced in the next section. The general Heisenberg Hamiltonian, H, is often written as[1-3]:

$$H = -\sum_{i,j}\left[J_{i,j}\left(S_i^x S_j^x + \gamma\left(S_i^x S_j^x + S_i^y S_j^y\right)\right)\right] \qquad (1)$$

where we restrict ourselves to nearest neighbor interactions (i,j represents a sum over nearest neighbor pairs of spins), allow for the exchange interaction to differ between pairs of spins in differing crystallographic directions, and allow for the spin to vary from Heisenberg-like ($\gamma = 1$) to Ising-like ($\gamma = 0$).

Equation 1 has been used for extensive study of magnetic phenomena in crystalline systems. Since the high T_C molecular based magnets are disordered we examine how the basic Heisenberg Hamiltonian can be modified to account for the effects of the randomness. Assuming the average spin-spin interaction is isotropic (Heisenberg) Eq. 2 incorporates the effects of exchange and the effects of random anisotropy[12,13]:

$$H = -\sum_{i,j} J_{i,j}\vec{S}_i \cdot \vec{S}_j - D_r\sum_i\left(\hat{n}_i \cdot \vec{S}_i\right)^2 - D_c\sum_i\left(\hat{N}_i \cdot \vec{S}_i\right)^2 - g\mu_B\sum_i \vec{H}\cdot\vec{S}_i \qquad (2)$$

Here the first term represents the average exchange interaction, the

second term represents a random magnetic anisotropy (D_r), the third a constant magnetic anisotropy (D_c) and the fourth is the Zeeman term representing interaction with an applied magnetic field. One approach assumes that the magnetic order is determined by the random exchange[12,13], assuming $D_c < D_r << J_{ij}$. In this event, a correlated spin glass occurs for $D_c << D_r$ while a ferromagnet or ferrimagnet with wandering axis occurs for large D_c or large Zeeman term. An alternate approach neglects the effects of random anisotropy and assumes that the magnetic order is determined by random exchange only[14].

METALLOCENE/ACCEPTOR SYSTEMS

The decamethylmetallocene molecule [MCp^*_2], Fig. 1a, provides a building block that enables one to prepare a wide variety of essentially isostructural materials while varying only the spin per metallocene repeat. Depending upon the choice of metal ion sandwiched between the two $C_5(CH_3)_5$ planar moieties, the spin per cation varies from S = 0 (for $[CoCp^*_2]^+$) to S = 3/2 (for $[CrCp^*_2]^+$). In principal, similar cations of controlled spin can be made incorporating other metal atoms between two C_6-rings. The electronic structure shown schematically in terms of only the metal d level contributions of the metallocence cations with differing metals are in Fig. 2.

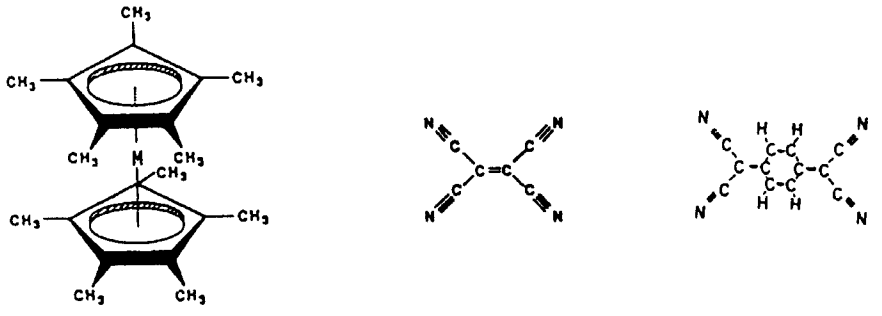

(a) (b) (c)

Fig. 1. (a) MCp*2, (b) TCNE, and (c) TCNQ.

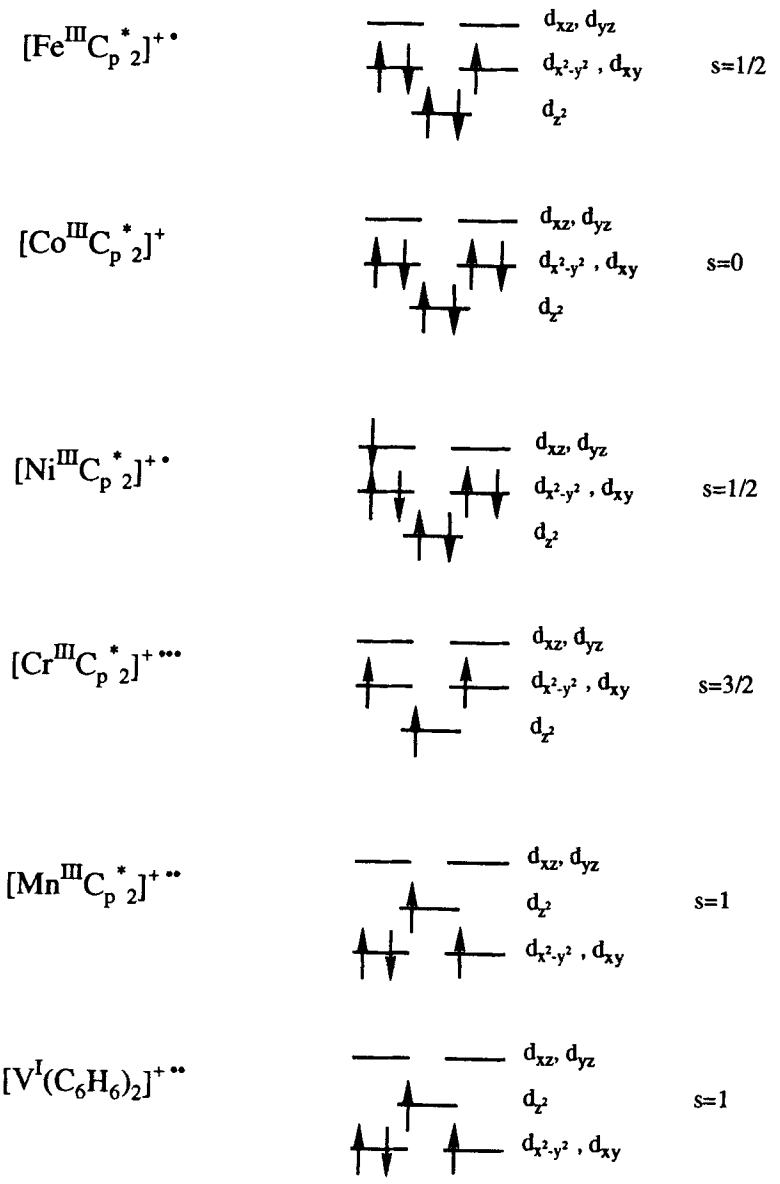

Fig. 2. Schematic illustration of electronic energy levels and spin values for metallocene cations with differing metal ions. In differing environments the energy levels may order differently.

Quasi-one-dimensional linear chain crystal structures of alternating cations and anions often form when the 1:1 electron transfer salts are prepared from $[MCp^*_2]$ and acceptors such as TCNE (tetracyanoethylene, Fig. 1b), TCNQ (7,7,8,8-tetracyano-p-quinodimethane, Fig. 1c), and DDQ (2,3-dicyano-5,6-dichloroquinone).[15]

The $[MCp^*_2]$ salts display a wide variety of magnetic phenomena reflecting the strong anisotropy in the exchange that occurs due to the crystal structure and the spin distributions of the molecular components. In general at high temperatures their magnetic behaviors can be analyzed interms of the usual mean field Curie-Weiss law

$$\chi = \frac{C}{(T - \vartheta)} \qquad (3)$$

with C the Curie constant ($= Ng^2\mu_B^2S(S+1)/3k_BT$) where N is the number of moles of spin S, g the Lande gyromagnetic ratio, μ_B the Bohr magneton, k_B the Boltzmann constant, and θ the Curie-Weiss temperature. At low temperature the magnetic response deviates from the mean field prediction usually following a one-dimensional-like behavior. Finally three-dimensional ferromagnetic or antiferromagnetic ordering occurs. It is noted that while 3-D ordering is related to the exchange and spin magnitude in mean field[1,2,16] as

$$T_C = 2JzS(S+1)/3k_B \qquad (4)$$

where z is the number of nearest neighbor spins, for a nearly one-dimensional material, T_C is substantially reduced[17]:

$$T_C = b(J_\parallel|J_\perp)^{1/2} \qquad (5)$$

where b depends upon the details of the crystal structure (for example, b = 1.556 for a tetragonal structure[17]).

Through choice of cation and anion one can explore a wide variety of magnetic phenomena which in turn give insight into the chemical control of magnetism in the molecular/polymeric state. Also the systematic substitutions for donors and acceptors allow for tests of a number of models proposed for the origin of the magnetic exchange in molecular/polymer magnets. Selected aspects of experiments are summarized here.

Models for magnetic exchange in molecular/polymeric magnets

In principal the origin of magnetic exchange is in the Pauli exclusion principle and its application to the electronic energy levels of a solid, As the electronic states of molecular systems are discrete and the band structures for polymers relatively simple there has been considerable discussion[10,11] concerning how to apply this principle to the molecular/polymeric solids to obtain ferromagnetic coupling among sites with unpaired spins.

Among models that have been proposed for magnetic exchange in these systems is configuration mixing of virtual triplet excited states with a ground state for D^+A^- alternating chains (degenerate Hubbard model)[18,19], very high spin multiplicity radicals[20], Heitler-London spin exchange between positive spin density on one radical and negative spin density on another[21a], Coulomb correlation between electrons in orthogonal orbitals (Hund's rule)[21b], antiferromagnetic exchange (by virtural excitation) between localized d electron spins of the metallocene radicals and delocalized π electrons of the $TCNE^{-\cdot}$ and Cp^- rings[22], superexchange (spin polarization) through a filled orbital of a closed shell molecular ion (e.g., Cp^-)[23] and through space dipolar interactions[24].

Though the configuration mixing model has been successful in explaining much of the data on the metallocence electron transfer salts and may account for the ferrimagnetic ground state of $V(TCNE)_x \cdot y$(solvent), it fails to account for the sign of the exchange in some circumstances (such as $[CrCp^*_2][TCNE]$[25] and $[CrCp^*_2][TCNQ]$[26]). Different models may need to be applied to determining the exchange in differing directions in a particular crystal structure. It is noted that the exchange interaction is rarely calculated for conventional inorganic magnets, where the sign and magnitude of the exchange are usually determined be experiment.

[FeCp*2][TCNE]: 3-D Molecular Ferromagnetism

The [FeCp*2][TCNE] system has a S = 1/2 spin on both the donor and the acceptor molecule. Above 16K the magnetic susceptibility behaves as expected for a 1-D ferromagnetically coupled Heisenberg chain.[6] Below that temperature, the susceptibility diverges as $(T-T_C)^{-\gamma}$ as expected for a Heisenberg like system approaching a 3-D ordered state. Spontaneous magnetization below T_C - 4.8K roughly follows $(T_C - T)^{\beta}$ with $\beta \sim 0.5$. Hysteresis loops are well defined, Fig. 3, with the coercive field H_C = 1000G at 2K indicating strong pinning of the domain walls.

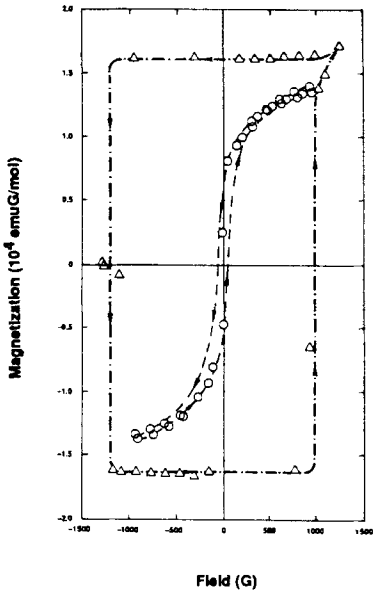

Fig. 3. Magnetization M as a function of applied filed H for [FeCp*2][TCNE]. (from Ref. 6)

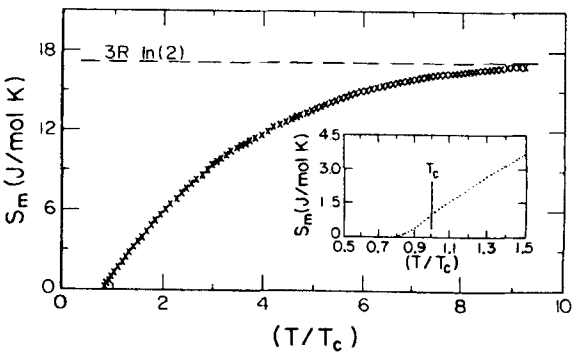

Fig. 4. Magnetic entropy vs reduced temperature, T/Tc, for [FeCp*2][TCNE]. Inset shows entropy vs T/Tc in the vicinty of Tc. (from Ref. 27)

Specific heat provides a direct measure of the one-dimensionality of the system[27]. As can be seen in Fig. 4, most of the entropy (96%) involved in ordering of the spins occurs above the 3-D transition temperature, with only 4% involved in ordering below T_c. Using as J the exchange (27K) determined by fitting the 1-D Heisenberg model to the susceptibility above T (for magnetic fields parallel the stack axis) and Eq. 6 for an anisotropy magnet, $J_\perp$ = 0.35K, leaving a ratio of $J_\parallel/J_\perp$ = 77.

[FeCp*2]x[CoCp*2](1-x)[TCNE]: Spinless defects and Suppression of T_c

The ability to controllably dope spinless $[CoCp^*_2]^+$ into the ferromagnetically coupled chain compound $[FeCp^*_2][TCNE]$ enables the controlled insertion of spinless sites into the magnetic chain[28,29]. Since, as noted above, the developments of substantial 1-D magnetic order along the chains precedes the 3-D ordering, spinless sites are expected to have a dramatic effect upon the 3-D ordering.

The rapid reduction of T_c as a function of the fraction of spinless metallocene sites (1-x) is plotted[29] in Fig. 5. For example, replacement of 2.5% of the S = 1/2 $[FeCp^*_2]$ sites by S = 0 $[CoCp^*_2]$ sites decreases T_c by 43%. The inset presents the results of a calculation[30] of the predicted decrease of T_c as a function of the fraction of sites with spin for varying ratios of inchain to interchain exchange in the limit of Ising spins. The experimental data are in concordance with a ratio of intrachain to interchain exchange of ~30:1.

The experimental results for the $[FeCp^*_2]_x[CoCp^*_2]_{(1-x)}[TCNE]$ system demonstrate the critical importance of 3-D coupling and long chain length in creating molecular/polymeric materials that have spontaneous magnetic order. Thus for example, finite oligomers that are only weakly coupled to each other are not expected to show a significant temperature for 3-D magnetic ordering.

[MnCp*2][TCNE]: Effects of Spin Magnitude on T_c

The ability to substitute S = 1 $[MnCp^*_2]^+$ cation for the S = 1/2 $[FeCp^*_2]^+$ cation enables a test of the role of spin magnitude in determining T_c.

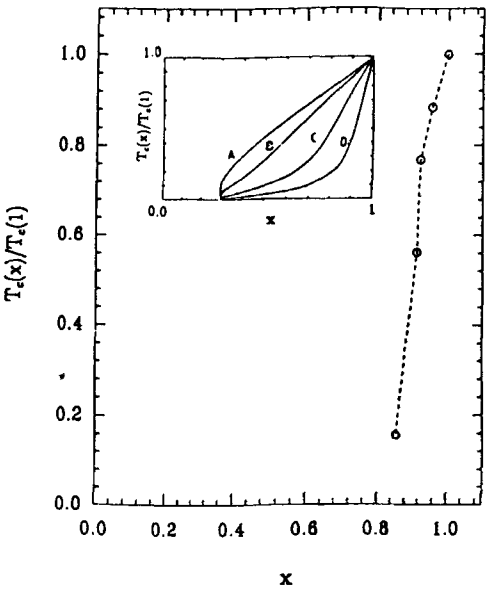

Fig. 5. Tc(x)/Tc vs x for [FeCp*2]x[CoCp*2](1-x)[TCNE] (from Ref. 29). The inset is the results of a calculation for Ising spins. The ratio of interchain to intrachain coupling is 1 (A), 0.1 (B), 0.02 (C), and 0.005 (D) (from Ref. 30).

Mean field models predict[31] an increase of T_C of a factor of 1.87. This is nearly exactly that which was experimentally determined[32] for [$MnCp^*_2$][TCNE]. However, it is noted that its Curie-Weiss θ actually smaller than that for [$FeCp^*_2$][TCNE] (H parallel the stacking axis) pointing to caution in the application of mean field scaling formulas.

It is noted for comparison that while [$FeCp^*_2$][TCNQ] is metamagnetic with an antiferromagnetic T_C= ~2.55K, (likely ferromagnetic coupling in the chain direction, antiferromagnetic coupling in the perpendicular direction)[33]. [$MnCp^*_2$][TCNQ] is ferromagnetic with a T_C of 6.2K[34]. Hence not only is there in increase in the T_C with increase of the S of the donor, there is also a change in the sign of the interchain exchange. Thus a full accounting of the spin interactions is necessary for any accurate scaling.

The S = 3/2 $[CrCp^*_2]^+$ cation when incorporated into the same structure type to form [$CrCp^*_2$][TCNE] is also ferromagnetic[25] (as is too

the $[CrCp^*_2][TCNQ]$[26]) though its T_c is only ~3.6K, contrary to expectations of a further increase in T_c with increasing S. No hysteresis loop is observed for the $[CrCp^*_2]^+$ compounds. An additional cation orbital perhaps is involved for the $[CrCp^*_2]^+$ compounds; this may be related to the origin of the reduced T_c's.

[MnCp*2][DDQ]: Weak interchain antiferromagnetic exchange and metamagnetism

In contrast to $[MnCp^*_2][TCNE]$[32] and $[MnCp^*_2][TCNQ]$[34] which both have a transition to a 3-D ferromagnetic ground state (at 8.8K and 6.2K respectively), the $[MnCp^*_2][DDQ]$ at low applied magnetic fields has an 8.5K transition to an antiferromagnetic ground state[35,36]. The systematic decrease (increase) of the ferromagnetic (antiferromagnetic) interchain interaction as the anion increases in size from TCNE to TCNQ to DDQ suggests that these anions have a net antiferromagnetic interaction with each other (as expected for the configuration mixing model because these anion radicals all have a nondegenerate partly occupied orbital). The progression from ferromagnetic $[FeCp^*_2][TCNE]$ (T_c = 4.8K[6]), to antiferromagnetic (at zero applied field - metamagnetic at higher fields) $[FeCp^*_2][TCNQ]$[33], to not magnetically ordered $[FeCp^*_2][DDQ]$[37,38] follows a similar trend.

At sufficiently large applied magnetic fields ($\mu_B H \sim J_\perp$) the weak antiferromagnetic interchain exchange interaction can be overcome giving rise to metamagnetism as observed for both the $[MnCp^*_2][DDQ]$ (at ~800Oe)[35,36] and the $[FeCp^*_2][TCNQ]$ (at ~1600 Oe)[33] systems.

$V(TCNE)_x \cdot ySOLVENT$: HIGH T_C MOLECULAR BASED MAGNETS

The success in developing new magnetic materials based on the decamethylmetallocene/TCNE framework and the achievement of higher T_c's through use of S = 1 $[MnCp^*_2]^+$ lead to the attempt at preparing analogous higher spin linear chain electron transfer salts using bis(benzene)vanadium as the donor molecule[7]. (As shown

schematically in Fig. 2, its cation state has the same electronic structure and the same S = 1 as the $[MnCp^*_2]^+$ cation.)

Sample preparation, composition and local order

To prepare the material TCNE and $V(C_6H_6)_2$ were separately dissolved in spinless organic solvents (CH_2Cl_2, CH_3CN, C_4H_8O, C_6H_6, ...). Upon mixing dropwise a precipitate forms immediately[7,9]. The samples then were stored under vacuum to remove excess solvent. The material resulting from preparation in CH_2Cl_2 has the hysteresis loop at room temperature with a coercive field of ~60G, Fig. 6, demonstrating that a room temperature molecular based magnet has been achieved[7].

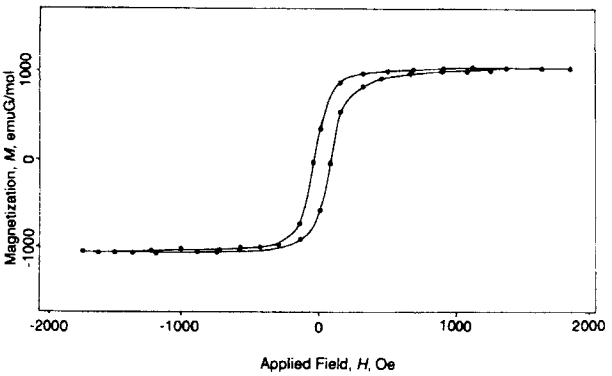

Fig. 6. Hysteresis loop, M vs H, at room temperature for V(TCNE)x.y(CH2Cl2). The line is a guide to the eye. From Ref. 7 (Copyright 1991 by the AAAS).

Chemical analyses determine that the stoichiometry is variable. Representing the materials as $V(TCNE)_x{\cdot}y(solvent)$ yields typical values of x ~ 2, and y ~1/2. There is no indication of any C_6H_6 in the precipitate. In agreement with the variable stoichiometry, powder x-ray diffraction measurement show the presence of several broad diffraction peaks indicating a disordered material with a typical coherence length of ~15Å[39] for material prepared in CH_2Cl_2. Preliminary x-ray diffraction studies indicate that the amount of order decreases when THF (C_4H_8O) is the solvent, while the samples are nearly amorphous when acetonitrile (CH_3CN) is used as the solvent[40].

The C-N stretching frequency points to the TCNE being a monoanion and hence having spin 1/2. From the average stoichiometry

and the usual saturation moment (see below) it is assumed that the vanadium is in the V^{+2} oxidation state with spin 3/2. Because V^{+2} usually has octahedral symmetry it is expected to coordinate with up to six TCNE and/or solvent molecules. Similarly the TCNE may coordinate with up to four V^{2+} because of their four C-N groups.

Ferrimagnetic ordering in $V(TCNE)_x \cdot y(Solvent)$ and mechanism of exchange

The temperature dependence of the magnetization of $V(TCNE)_x \cdot y(CH_2Cl_2)$ determined at a number of different applied fields (up to 19.6 kG), Fig. 7, shows a saturation magnetization of ~5300 emuG/mol at 4.2K. The value

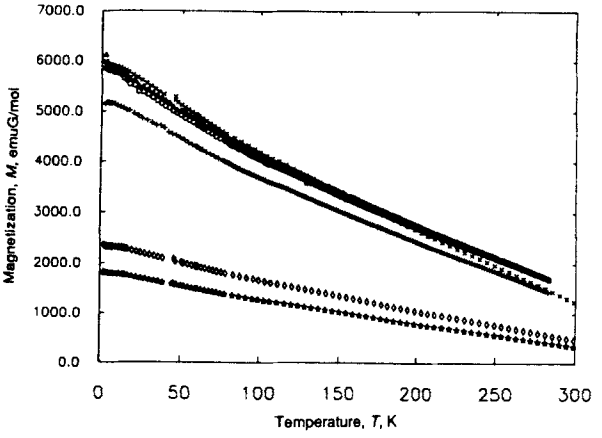

Fig. 7. M vs T at 0.15, 0.5, 2.0, 5.25, 15.8, and 19.5 kG for V(TCNE)x.y(CH2Cl2). From Ref. 7 (Copyright 1991 by the AAAS).

is substantially lower than expected for ferromagnetic ordering of the S = 3/2 V^{2+} and S = 1/2 $TCNE^-$, but in agreement with the value expected for antiferromagnetic coupling of the V^{2+} spins and the $TCNE^-$ spins. In the latter case a stoichiometry of V:TCNE of 1:2 leads to a ferrimagnet with net spin 1/2 per formula unit and M_S of ~5500 emuG/mol.

The antiferromagnetic exchange coupling J may have its origin in configuration interaction (virtual charge transfer from V^{2+} to $TCNE^-$ or the reverse). For either direction of charge transfer antiferromagnetic alignment of the V^{2+} and $TCNE^-$ spins is required by

the Pauli exclusion principle, Fig. 8. For this scheme the effective exchange would then be given by the sum of the contributions of both forward (V^{2+} to $TCNE^{-}$: the energy cost of an excitation being ΔE_{VT}) and reverse ($TCNE^{-}$ to V^{2+}: the energy cost of an excitation being ΔE_{TV}) charge transfer. Using the Hubbard model[6], the effective Heisenberg exchange is then $J = 2t2[(1/\Delta E_{VT}) + (1/\Delta E_{TV})]$ where t is the transfer integral between the $TCNE^{-}$ b_{3g} orbital and the V^{2+} d levels.

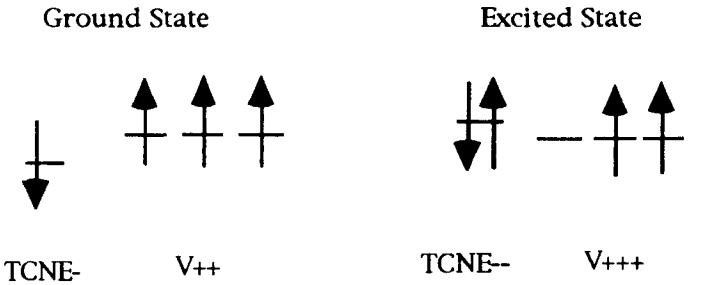

Fig. 8. Schematic illustration of possible charge transfer mechanism for antiferromagnetic exchange among V dications (S=3/2) and TCNE anions (S=1/2). Similarly an antiferromagnetic alignment occurs when forming the [TCNE (neutral) ; V(+1)] back charge transfer excited state.

<u>$V(TCNE)_x \cdot y(CH_2Cl_2)$: M(T) and determination of T_c</u>

The temperature dependent remanent magnetization of $V(TCNE)_x \cdot y(CH_2Cl_2)$ was determined by cooling the sample in an applied magnetic field to 2K then reducing the applied magnetic field to zero and monitoring M(T) as the sample warmed to room temperature. The result[41], Fig. 9, differs substantially from the usually expected behavior for crystalline magnets[42]. The nearly linear decrease of M(T) with increasing T for T>100K is more typical of disordered materials where there are fluctuations in the magnetic exchange values and/or the

magnetic anisotropy[12-14,42]. A linear extrapolation of the M(T) to $M(T_C) = 0$ leads to an estimate[41] of $T_C = 400K$.

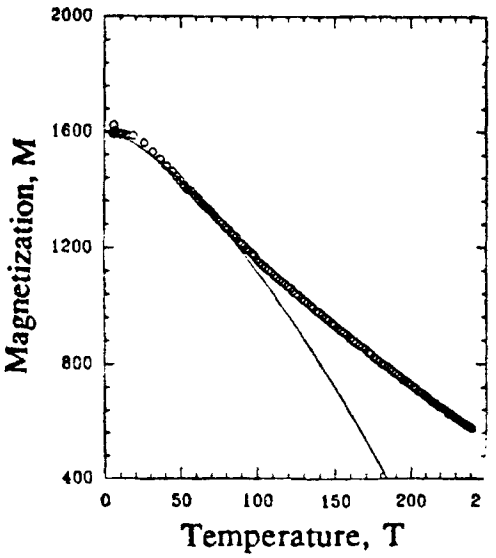

Fig. 9. T-dependent remanent magnetization of V(TCNE)x.y(CH2Cl2). The solid line is a fit to spin wave theory. See text. (from Ref.41)

The low temperature data may be analyzed using spin wave theory, which is usually applicable in the long wave length limit even in the presence of disorder[42]. Assuming

$$M_S - M(T) = BT^{3/2}$$

with the coefficient B related to the spin wave dispersion by $B \sim D^{3/2}$ where $E(k) = Dk^2$ (k is the wavevector for the spin waves), we estimate[41] that $D \sim 75$ meVÅ^2. Using the correlation between T_C and D developed for disordered magnets[42], this fit implies $T_C = 400K$, in remarkable agreement with the value determined by linear extrapolation of M(T) discussed above.

These estimates of T_C can be used to determine a value for the average exchange J. Using Eq. 4 for three-dimensionally coupled magnets, and assuming there are an average of five nearest neighbors as well as an effective spin value S(S+1) determined by by the root mean square value $[(1/2)(3/2)(3/2)(5/2)]^{1/2}$, $J = 70K$. This is only 2.6 times the intrachain exchange determined[6] earlier for $[FeCp^*_2][TCNE]$. The two

order of magnitude increase in T_c as compared to T_c of $[FeCp^*_2][TCNE]$ is in largest part due to the three-dimensional network increasing T_c by a factor of the number of near neighbors, in contrast to a quasi-one-dimensional chain system where T_c is reduced by the root mean square value of the inchain and interchain exchange (Eq. 5).

The sizable coercive field of disordered $V(TCNE)_x \cdot y(CH_2Cl_2)$ suggests significant fluctuations in the local magnetic anisotropy field as might be expected[42] in a system with considerable disorder.

Effect of solvent on magnetism

In order to gain insight into the magnetic state, samples prepared in several different solvents were studied, with particular emphasis on CH_2Cl_2, THF (C_4H_8O), and acetonitrile (CH_3CN). The ac susceptibility measured[43] at 400 Hz for typical compositions obtained from these solvents is shown in Fig. 10. The $V(TCNE)_x \cdot y(CH_2Cl_2)$ system has a T_c in excess of room temperature. The decrease in χ_{ac} below 100K likely reflects the increasing domain wall stiffness of this ferrimagnet as T is decreased. In contrast, χ_{ac} of samples prepared in THF have T_c of ~180K with a constant ac susceptibility at lower temperatures consistent with w e a k o r

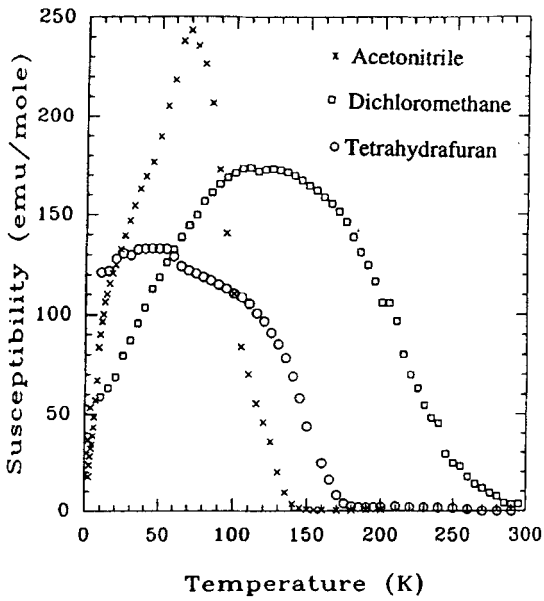

Fig. 10. Ac susceptibility vs temperature for V(TCNE)x prepared in CH2Cl2, THF, and acetonitrile. (from Ref.43)

absent coercive field. Acetonitrile prepared samples have an even lower T_C (ranging from ~60K to ~150K), with a relatively sharp maximum in the χ_{ac} and a decrease in χ_{ac} at lower temperatures) reminiscent of reentrant spin glass like behavior (typically the spin glass freezing temperature, T_f, for acetonitrile prepared samples is ~15K). The broad range of its T_C suggests the critical role of variations in local composition for this system.

V(TCNE)$_x$·y(CH$_3$CN); Effects of fluctuation in local anisotropy ($D_T \geq D_C$)

We have extensively studied[44] the V(TCNE)$_x$·y(CH$_3$CN) acetonitrile samples to gain insight into the origins of the magnetism in these materials. The positive slope of the plot of χ*T vs. T for T>200K, Fig. 11, is typical of ferrimagnetic materials at temperatures greater than the ordering temperature. This positive slope reflects that the primary exchange present in the material is antiferromagnetic, while the rapid increase in the product χ*T below 150K shows the effects of three-dimensional magnetic ordering in this material. The magnetization measured at varying applied fields is plotted in Fig. 12. Similar to the behavior of the CH_2Cl_2 prepared samples, the M(H,T) is very different from that of the usual crystalline magnets with a very strong field dependence and an unusual nearly linear temperature dependence.

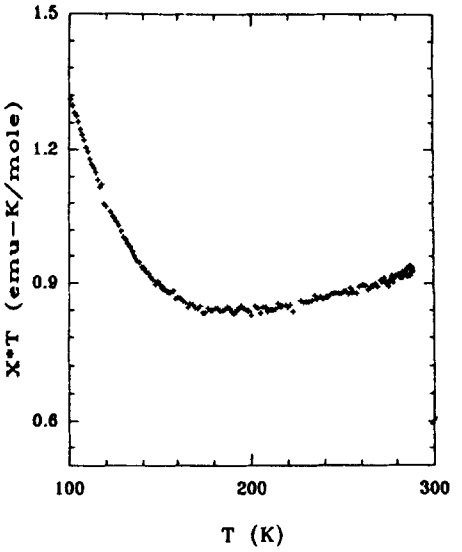

Fig. 11. X*T for V(TCNE)x.y(CH3CN). (from Ref. 44)

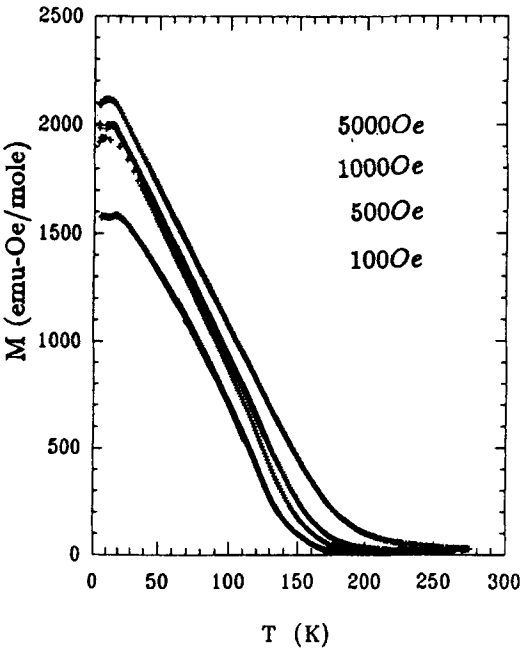

Fig. 12. M vs T at 0.1, 0.5, 1.0 and 5.0 kG for V(TCNE)x.y(CH3CN). (from Ref. 44)

Given that there is a substantial disorder in the material, and that the spinless CH_3CN will tend to coordinate with V^{2+} displacing the S=1/2 $[TCNE]^{-\cdot}$, we examined the data in light of available models for the effects of disorder on magnetism. The randomness in coordination and order are expected to lead to some variation in the magnitude of the exchange between the S=3/2 V^{2+} and the S=1/2 $[TCNE]^{-\cdot}$, although the sign of the exchange is expected to remain constant. More importantly, the disorder is expected to lead to variation in a small anisotropy as spinless CH_3CN molecules displace some of the S=1/2 $[TCNE]^{-\cdot}$. This suggests the application of models based on Eq. 2 with the effects of random anisotropy being primary.

Given the behavior of the CH_2Cl_2, THF and CH_3CN materials, we suggest that for the CH_2Cl_2 system the constant magnetic anisotropy term exceeds the random term ($D_c > D_r$) and that its magnetic properties are that of a ferrimagnet with wandering axis (FWA); that for the THF system the constant anisotropy and random anisotropy are of the same order ($D_c \sim D_r$); and that for the CH_3CN system the random anisotropy

exceeds that of the constant anisotropy ($D_r > D_c$) and that its magnetic properties are those of a reentrant correlated spin glass. The magnetic properties of the THF system are intermediate between those of the CH_2Cl_2 and the CH_3CN systems. This behavior correlates with the CH_2Cl_2 being the least coordinating of the three solvents with the THF coordinating more easily and the CH_3CN being the most readily coordinating solvent. This also correlates with the CH_2Cl_2 system being the least disordered, with the THF and CH_3CN systems having increasing disorder respectively[39,40]. In light of this we analyze the low temperature data for the CH_3CN material in the random anisotropy model of Chudnovsky[12,13] with the behavior near the three-dimensional ordering temperature T_c analyzed within the modified equation of state analysis of Aharony and Pytte[45] and also Gehring, et al.[46]

$V(TCNE)_x \cdot y(CH_3CN)$: Low Temperature Magnetization

The magnetic field dependent magnetization of $V(TCNE)_x \cdot y(CH_3CN)$ measured at 4.2K is shown in Fig. 13. The relatively slow approach to saturation of M(H) is unusual for a magnetic material and suggests the critical role of disorder and random anisotropy. The model of Chudnovsky[12,13] predicts that M(H) increases as $(H+H_c)^{1/2}$ for $D_r > D_c$ and $D_r << J$, where H_c is the coherent anisotropy field. The solid line in Fig. 13 is a quantitative fit to the data with $H_c \sim 21$kG. This value of H_c is only about 2% of the value of J, self-consistent with the model that the system is in an weak anisotropy regime.

$V(TCNE)_x \cdot y(CH_3CN)$: Critical exponents near T_c

The behavior near T_c can be analyzed using a modified equation of state approach to obtain effective critical exponents for this disordered magnetic system. A critical isotherm can be determined[44] by plotting M(H) vs H at varying temperatures, with M proportional to $H^{1/\delta}$ at T_c.. Using this analysis we determine that $\delta = 4$ and $T_c = 135$K for a typical sample studied. With T_c and δ determined, exponents β_a and γ_a can be determined directly by analyzing isothermal plots of $(H/M)^{1/\gamma_a}$ vs. M^{1/β_a}. Given β_a and δ all of the M(H,T) data in the vicinity of T_c can be collapsed onto a single set of curves for plots of $\ln(M/|t|^{\beta_a})$ vs. $\ln(H/|t|^{\beta\delta})$

where t = $|T-T_C|$, Fig. 14. The lower curve corresponds to $T>T_C$ and the upper curve corresponds to $T<T_C$.

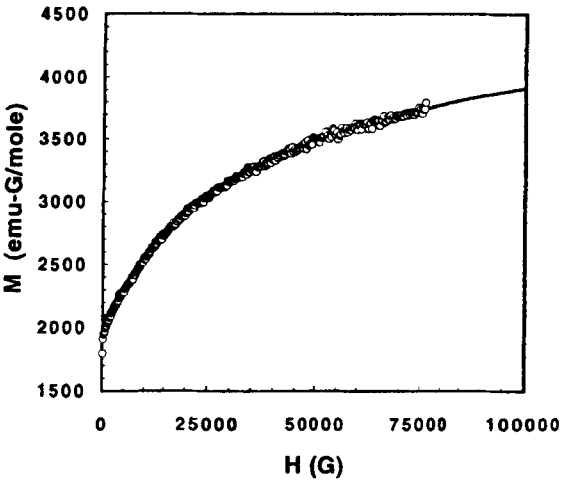

Fig. 13. Magnetic field dependence of M at 4.2K for V(TCNE)x.y(CH3CN). The solid line is a fit to the random anisotropy model. (from Ref. 44)

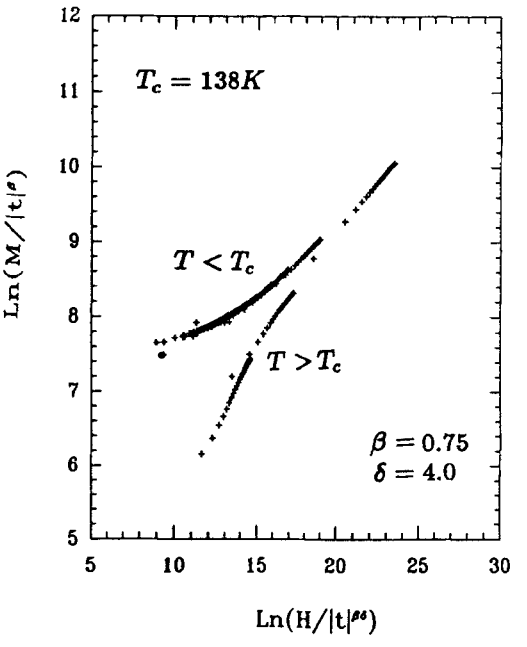

Fig. 14. Scaling plot of for V(TCNE)x.y(CH3CN) with Tc = 138K (see text). (from Ref. 44)

V(TCNE)$_x$·y(THF): Effects of fluctuation in local anisotropy ($D_r \sim D_c$)

The magnetic properties of V(TCNE)$_x$·y(THF) are intermediate between those of the CH_2Cl_2 and CH_3CN derived samples[47]. The temperature dependent magnetization at differing magnetic fields, Fig. 15, again shows the quasi-linear behavior below $T_c \sim 210K$, with an unusually strong magnetic field dependence below T_c indicative of the presence of disorder. There is an upper limit on the coercive field of 10G. The results have been interpreted in terms of the model of dominant effects of random magnetic anisotropy, with comparison to the theory of Chudnovsky[12,13] at low temperatures. The M(T) increases at low temperature (inset of Fig. 15), perhaps indicative of superparamagnetic coupling[47].

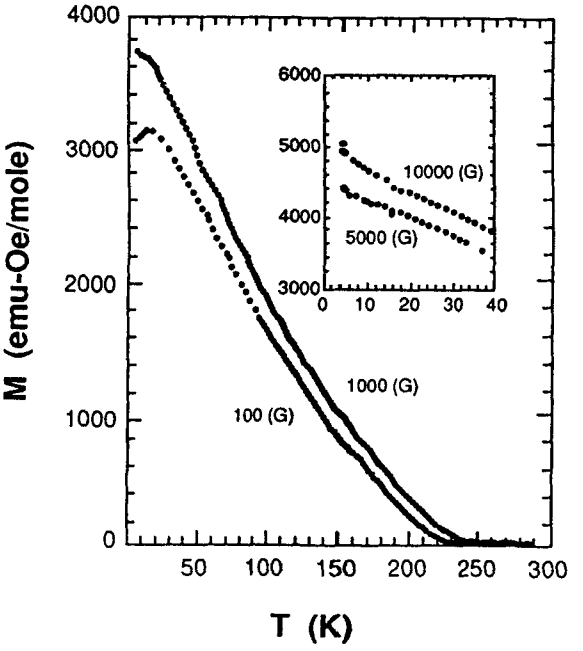

Fig. 15. M vs T at 0.1 and 1.0 kG for V(TCNE)x,y(THF). The inset shows data for 5.0 and 10.0 kG. (from Ref. 47)

Equation of state analyses of isotherms near T_c show a strong fluctuation of local magnetization and yield relatively large values of critical exponent as compared to those expected for the usual three-

dimensional systems with long range order. The scaling plot obtained for T_C = 210K is given in Fig. 16.

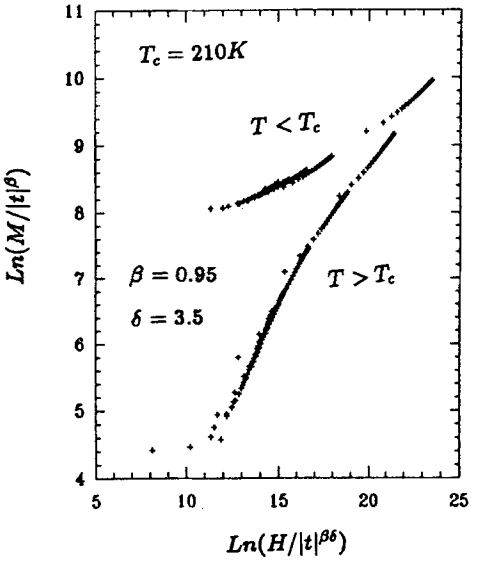

Fig. 16. Scaling plot for V(TCNE)x.y(THF) using Tc = 210K. (from Ref. 47)

Electron Paramagnetic Resonance: A flexible probe of unusual phenomena

The electron paramagnetic resonance of $V(TCNE)_x{\cdot}y(solvent)$ has been studied[48] for CH_2Cl_2, THF and CH_3CN solvents. A rich set of temperature dependent spectra give insight into the magnetism. A typical derivative spectrum at room temperature for $V(TCNE)_x{\cdot}y(CH_2Cl_2)$ is shown in Fig. 17.

Four distinct features are observed[48], (1) the main resonance with g~1.92, (2) an approximately half-field resonance, (3) a broad near zero field resonance, and (4) a narrow zero field antiresonance. These features vary systematically with samples composition (including differing solvents) and temperature. The latter two features at 200K are more clearly shown in Fig. 18. The integrated intensity of the main resonance for each of the compositions studied scales with the measure temperature dependent dc magnetization, hence it is associated with the ferrimagnetic resonance. Contrary to the usual magnetic systems, the linewidth reaches a minimum at T_C, with a critical behavior mimicking the critical behavior of M(T), as expected for a material with 'sloppy'

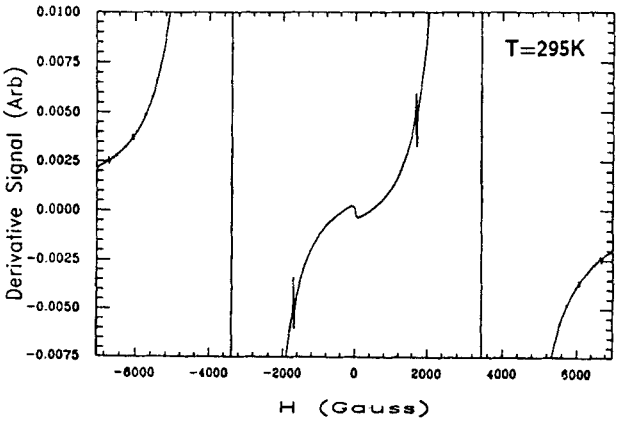

Fig. 17. Derivative EPR signal vs H for V(TCNE)x.y(CH2Cl2) at 295K. (from Ref. 48)

spin waves (spin waves with wave vector $q > \xi$, where ξ is the correlation length[49]). The g-shift of the main resonance line scales with the magnetization and agrees in magnitude with expectations of demagnetization effects.

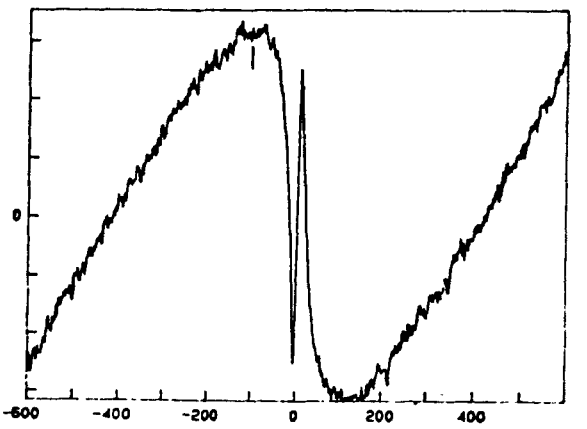

Fig. 18. Near zero field EPR signal of V(TCNE)x.y(CH2Cl2) at 200K. (from Ref. 48)

The broader low field signal is largest in the CH_2Cl_2 prepared materials, weak in the THF prepared systems and virtually non-existent in the CH_3CN prepared materials. The peak to peak width and its sample variation suggest that it is a domain wall like resonance. The sharp zero field signal is unusual. It is present in each of the compositions below T_c though for the CH_3CN prepared samples it evolves into a resonance from an antiresonance below ~15K, a temperature associated with freezing out of the spins into a spin glass phase. Based on this temperature dependence this antiresonance may be caused by a low field magnetoresistance making it more difficult for electrons to hop among charge carrier sites (presumably TCNE) thereby reducing the sample absorbance of microwaves at higher magnetic fields.

V(TCNE)$_x$·y(solvent) conductivity; correlated hopping

The V(TCNE)$_x$·y(solvent) materials have moderate conductivites of order 10^{-5} to 10^{-3} S/cm at room temperature, depending upon the solvent[50]. In general the dc conductivity varies as $\exp[-(T_0/T)^{1/4}]$ reminiscent of Mott variable range hopping[51]. The frequency (f) dependence, Fig. 19, suggests that the behavior is more complex[50,52]. The frequency dependent component of the conductivity varies as f^sT^n with s~0.7 typical of near-neighbor pairwise hopping. However, n~4 instead of 1, the value typical of polymers and amorphous semiconductors[53].

We suggest that this unusual temperature dependence of the conductivity at higher frequencies may be a reflection of the correlated spin glass behavior of the V(TCNE)$_x$·y(solvent) materials. The charge transport likely involves charge hopping among TCNE sites. (Because of its smaller size the Coulomb repulsion for an extra electron on V^{2+} is expected to be larger than that for an extra electron on the $TCNE^{-\cdot}$) If neighboring $TCNE^-$ sites have the spins aligned in the same direction, then an electron hop to a near neighbor requires an emission or absorption of a spin flip phonon to conserve total spin (since each of the near neighbor TCNE have their spins aligned in the same direction), while tunneling a distance greater than the magnetic correlation

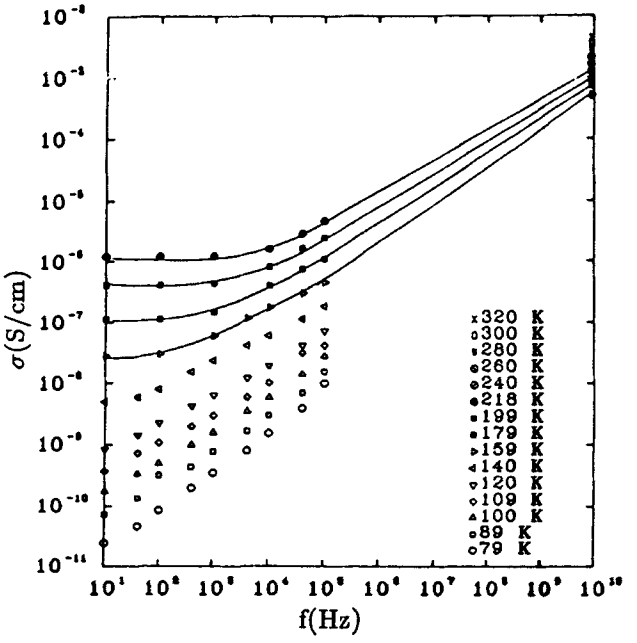

Fig. 19. The temperature and frequency dependence of conductivity of V(TCNE)x.y(CH2Cl2). (from Refs. 50 and 52).

l

ength results in an electron transition without the cost of the spin flip process. The probability p_i of electron transition between near and/or far sites may then be modified to reflect the magnetic correlation in the following manner:

$$p_i \sim \exp[-(\Delta E/k_BT - \alpha r - \Delta E_{sf}(r)/k_BT]$$

where ΔE is the typical difference in energy of adjacent sites, α^{-1} the decay length of the electron states involved in the charge transport, and $\Delta E_{sf}(r)$ is the distance r dependent energy required for flipping of spins to allow the electron transition. For sites separated by greater than the magnetic correlation length the spin flip energy term goes to zero.

SUMMARY

Molecular/polymer based magnets provide a framework for study of a wide variety of magnetic phenomena. The crystalline metallocene based electron-transfer salts are laboratories for the study of the competition

between one-dimensional and three-dimensional magnetic phenomena as well as model systems for the study of the mechanisms for magnetic exchange in molecular solids. In these systems T_C is suppressed from that expected for the $J_{\|}$ present due to the small interchain exchange.. Modest applied magnetic fields of order $J_{\perp}$ can lead to changes in magnetic state as in metamagnetism. Though virtual charge transfer among neighboring sites can account for the sign of the magnetic exchange in the great majority of systems studied, exceptions such as the $[CrCp^*_2][TCNE]$ system demonstrate that more than one mechanism for exchange is operative in these molecular systems.

The advent of the $V(TCNE)_x \cdot y(solvent)$ systems demonstrated that room temperature magnetism is achievable in molecular/polymeric materials. The nearly hundred fold increase in T_C is attributed to both an increase in J (due to closer approach of the spins) and three-dimensional coordination. Analysis of a variety of data demonstrates that the disorder in the material introduces a weak random anisotropy which in turn determines whether the material is in a three-dimensional magnetic state (even at room temperature), a low temperature magnet, or even a spin glass. Control of the local order, structure, spin, and chemical composition determines the magnetic state achieved and its charge transport and dynamic properties.

ACKNOWLEDGMENT

The authors thank their colleagues, postdoctoral fellows, students, and visiting scientists that have contributed so much to the studies presented here. Specials thanks are extended to G. Du, J. Joo, M. Laridjani, S. Long, R.S. McLean, B.G. Morin, K.S. Narayan, Z. Oblakowski, J.P. Pouget, S. Zane, P. Zhou, and F. Zuo for allowing us to report work in progress. This research was supported in part by the U. S. Department of Energy Division of Materials Sciences Grant DE-FG02-86ER45271.A.

REFERENCES

1. J.H. van Vleck, The Theory of Electric and Magnetic Susceptibilities, Oxford University Press, London (1932).
2. J.H. van Vleck, Rev. Mod. Phys. 25, 220 (1953); D.C. Mattis, The Theory of Magnetism I, Springer-Verlag, Berlin, 1981.
3. See, for example, Proc. 5th Joint Magnetism and Magnetic Materials-Intermag Conf., 18-21 June 1991, ed. by E.D. Dahlberg, D.T. Pierce, and W.B. Yelon (J. Appl. Phys. 70, No. 10, Pt. II (1991)).
4. J.S. Miller, P.J. Krusic, A.J. Epstein, W.M. Reiff, and J.H. Zhang, Mol. Cryst. Liq. Cryst. 120, 27 (1985).
5. J.S. Miller, J.C. Calabrese, H. Rommelmann, S. R. Chittipeddi, J.H. Zhang, W.M. Reiff, and A.J. Epstein, J. Am. Chem. Soc. 109, 769 (1987).
6. S. Chittipeddi, K.R. Cromack, J.S. Miller, and A. J. Epstein, Phys. Rev. Lett. 58, 2695 (1987).
7. J.M. Manriquez, G.T. Yee, R.S. McLean, A.J. Epstein, and J.S. Miller, Science 252, 1415 (1991).
8. A.J. Epstein and J.S. Miller, in Proc. Nobel Symp. NS-81 on Conjugated Polymers and Related Materials: The Interconnection of Chemical and Electronic Structure, June 1991, Lulea, Sweden, ed. by W.R. Salaneck, I Lunström, and B. Rånby (Oxford Univ. Press, London, 1993), p. 475.
9. J.S. Miller, G.T. Yee, J.M. Manriquez, and A.J. Epstein, in Proc. Nobel Symp. NS-81 on Conjugated Polymers and Related Materials: The Interconnection of Chemical and Electronic Structure, June 1991, Lulea, Sweden, ed. by W.R. Salaneck, I Lunström, and B. Rånby (Oxford Univ. Press, London, 1993), p. 461.
10. See, for example, Proc. Conf. on Ferromagnetic and High Spin Molecular Based Materials, ed. by J.S. Miller and D.A. Dougherty, (Mol. Cryt. Liq. Cryst. 176 (1989)).
11. See, for example, Proc. Conf. on Molecular Magnetic Materials, ed. by O. Kahn, D. Gatteschi, J.S. Miller, and F. Palacio (NATO ARW E198, Kluwer Academic Publishers, Amsterdam (1991)).
12. E.M. Chudnovsky, J. Appl. Phys., 64, 5770 (1988).
13. E.M. Chudnovsky, W.M. Saslow, and R.A. Serota, Phys. Rev. B, 33, 251 (1986).
14. I.Ya. Korenblit and E.F. Schender, in Spin Waves and Magnetic Excitations 2, ed. by A.S. Borovik-Romanov and D.K. Sinha (Elsevier Science Publisher, B.V. 1988), p. 109.
15. J.S. Miller and A.J. Epstein, Chem. Rev., 88, 201 (1988).
16. C. Kittel, Introduction to Solid State Physics, 5th ed., John Wiley & Sons, New York, NY, 1976.
17. S.H. Liu, J. Magn. and Mag. Matr., 82, 294 (1989).
18. H.M. McConnell, Proc. R.A. Welch Found. Chem. Res., 11, 144 (1967).
19. J.S. Miller and A.J. Epstein, J. Am. Chem. Soc., 109, 3850 (1987).

20. N. Mataga, J. Chem. Phys., 39, 1910 (1968); A.A. Ovchinnikov, Theor. Chim. Acta, 47, 297 (1978).
21. (a) H.M. McConnell, J. Chem. Phys., 39, 1910 (1963); (b) O. Kahn,. Structure and Bonding, 68, 89 (1987).
22. A.L. Tchougreeff and I.A. Misurkin, Chem. Phys., 153, 371 (1991).
23. A.L. Buchachenko, Mol. Cryst. Liq. Cryst., 176, 307 (1989); Z.G. Soos and P.C.M. Williams, Mol. Cryst. Liq. Cryst., 176, 369 (1989); C. Kollmar and O. Kahn, J. Chem. Phys., 96, 2988 (1992).
24. M. Tamura, Y. Nakazawa, D. Shiomi, K. Nozawa, Y. Hosokoshi, M. Ishikawa, M. Takahashi, and M. Kinoshita, Chem. Phys. Lett., 186, 401 (1991); J.S. Miller, D.T. Glatzhofer, R. Laversanne, T.B. Brill, M.D. Timken, D.J, O'Conner, J.H. Zhang, J.C. Calabrese, A.J. Epstein, S. Chittipeddi, and P. Vaca, Chemistry of Materials, 2, 60 (1990).
25. F. Zuo, S. Zane, P. Zhou, A.J. Epstein, R.S. McLean, and J.S. Miller, J. Appl. Phys., in press; P. Zhou, A.J. Epstein, F. Zuo, S. Zane, S. McLean, and J.S. Miller, to be published.
26. W.E. Broderick and B.M. Hoffman, J. Am. Chem. Soc., 113, 6334 (1991).
27. A. Chakraborty, A.J. Epstein, W.N. Lawless, and J. S. Miller, Phys. Rev. B, 40, 11422 (1989).
28. K.S. Narayan, K.M. Chi, A.J. Epstein, and J. S. Miller, J. Appl. Phys., 69, 5953 (1991).
29. K.S. Narayan, B.G. Morin, J. S. Miller, and A.J. Epstein, Phys. Rev. B, 46, 6195 (1992).
30. A. Mujeeb and R.B. Stinchcombe, J. Phys. C, 15, 3163 (1982).
31. D.A. Dixon, A. Suna, J.S. Miller, and A.J. Epstein, in Proc. Conf. on Molecular Magnetic Materials, ed. by O. Kahn, D. Gatteschi, J.S. Miller, and F. Palacio (NATO ARW E198, Kluwer Academic Publishers, Amsterdam (1991)), p. 171.
32. G.T. Yee, J.M. Manriquez, D.A. Dixon, R.S. McLean, D.M. Groski, R.B. Flippen, K.S. Narayan, A.J. Epstein, and J.S. Miller, Adv. Mater., 3, 309 (1991).
33. G.A. Candela, L. Swartzendruber, J.S. Miller, and M.J. Rice, J. Am. Chem. Soc., 101, 2755 (1979).
34. W.E. Broderick, J.A. Thompson, E.P. Day, and B.M. Hoffman, Science, 249, 410 (1990).
35. J.S. Miller, R.S. McLean, C Vazquez, G.T. Yee, K.S. Narayan, and A.J. Epstein, J. Mater. Chem., 1, 479 (1991).
36. K.S. Narayan, O.Heres, A.J. Epstein, and J.S Miller, J. Magn. Mag. Mat., 110, L6 (1992).
37. E. Gebert, A.H. Reis, Jr., J.S. Miller, H. Rommelmann, and A.J. Epstein, J. Am. Chem. Soc., 104, 4403 (1982).
38. J.S. Miller, P.J. Krusic, D.A. Dixon, W.M. Reiff, J.H. Zhang, E.C. Anderson, and A.J. Epstein, J.Am. Chem. Soc., 108, 4459 (1986).
39. M. Laridjani, J.P. Pouget, J.S. Miller, and A.J. Epstein, to be published.

40. Z. Oblakowski, A.J. Epstein, J.P. Pouget, and J.S. Miller , to be published.
41. P. Zhou, K.S. Narayan, B.G. Morin, J.S. Miller, and A.J. Epstein, to be published.
42. F.E. Luborsky, in Ferromagnetic Materials, ed. by E.P. Wohlfarth, 1, 452 (1980).
43. B.G. Morin, P. Zhou, C. Hahm, A.J. Epstein, and J.S. Miller, J. Appl. Phys., xx, xxx (1993).
44. P. Zhou, B.G. Morin, J.S. Miller, and A. J. Epstein, to be published.
45. A. Aharony and E. Pytte, Phys. Rev. Lett., 45, 1583 (1980); and Phys. Rev B, 27, 5872 (1983).
46. P.M. Gehring, M.B. Salamon, A. del Moral, and J.I. Arnaudas, Phys. Rev. B, 41, 9134 (1990).
47. P. Zhou, J.S. Miller, and A. J. Epstein, to be published.
48. S.M. Long, K.R. Cromack, J.S. Miller, and A. J. Epstein, to be published.
49. D.L. Huber, Phys. Lett. 37A, 285 (1971).
50. G. Du, J.S. Miller, and A. J. Epstein, to be published.
51. N.F. Mott and E. Davis, Electronic Processes in Noncrystalline Solids (Clarendon Press, Oxford, 1979).
52. J, Joo, J.S. Miller, and A. J. Epstein, to be published.
53. F. Zuo, M. Angelopoulos, A.G. MacDiarmid, and A.J. Epstein, Phys. Rev. B, 39, 3570 (1989).